IOSR Journal of Applied Chemistry (IOSR-JAC)
e-ISSN: 2278-5736.Volume 15, Issue 7 Ser. II (July 2022), PP 23-35
www.iosrjournals.org

Isosorbide based-PPV derivatives containing electron-rich group for optoelectronic applications

Habiba Zrida[1], Khaled Hriz*[1], Nejmeddine Jaballah[1], Mourad Chemek[2], Mustapha Majdoub[1]

[1]*Laboratoire des Interfaces et des Matériaux Avancés (LIMA), Faculté des Sciences de Monastir, Bd. de l'Environnement, 5019 Monastir, Université de Monastir, Tunisia*
[2]*Laboratoire de recherche : Synthèse asymétrique et ingénierie moléculaire de matériaux pour l'électronique organique, Faculté des Sciences de Monastir, Bd. de l'Environnement, 5019 Monastir, Université de Monastir, Tunisie.*
** Correspondence to K. Hriz.*

Abstract
*A backbone engineering study has been performed with isosorbide based organic semiconducting materials to modulate their physical and electronic properties through the incorporation of tetrazole groups. In this context, a novel polymer type PPV containing tetrazole groups was elaborated. It was prepared by chemical modification of cyano (CN) groups of the synthesized precursor polymer (**CN-PPVIs**) using click chemistry reaction. The structural, thermal and photophysical properties of the synthesized polymers were investigated and the structure-property correlations were established based on the conjugated system nature. The obtained results showed a significant effect on the solid-state morphology and the electronic properties. The absorption study demonstrated as well that the incorporation of the tetrazole units in the macromolecular chain of **Tet-PPVIs** considerably increased its optical gap and limited the π-π interactions between the conjugated systems in the solid state. The tetrazole group effect was also observed on the HOMO-LUMO energy levels. In fact, **TET-PPVIs** show higher electron affinity and lower ionization potential in comparison with **CN-PPVIs**. Density Functional Density (DFT) of polymers has been realized it showed a remarkable variation in geometry depending on the incorporation of the tetrazole group. An analysis by RDG was carried out on the optimized structures of polymers in order to prove the intramolecular interactions.*

Keywords: *Semi-conducting Polymers; Click chemistry; DFT calculation; Optical properties; Space-charge limited current (SCLC).*

Date of Submission: 09-07-2022 Date of Acceptance: 25-07-2022

I. Introduction

Conjugated polymers have been widely used in light-emitting diodes (LEDs)[1-3]because the optical properties of these materials can be easily tuned by chemical modification, allowing to obtain an emission over different ranges of the visible spectrum.

Indeed, color tuning can be accomplished by several means, including the introduction and the modification of a specific chromophore designed with appropriate electron donor or acceptor groups, since these changes will affect the band gap [4].

Moreover, many studies focused on a particularly developed conjugated polymer family, such aspoly(paraphenylene vinylene) (PPV), which was already functionalized on main-chain [5], side-chain[6] or both [7] in order to obtain higher efficient and more stable LEDs [8].

In addition, PPV-polymer derivatives withintrinsically high electron affinity are currently highly desirable, since they reduce the barrier for electron injection and make possible the use of more stable electrodes such as aluminum. This is the reasonthat theelectron withdrawing–CαN substituents have been attached either to the double bonds [9, 10]or to the aromatic ringsin order to increase the electron affinity of PPV[11]which allow to improve the electron transport properties [10]. Several conjugated polymers containing cyano groups such as poly(phenylenecyanovinylene)s [12],poly(N-alkyl-3,6-carbazole), and poly[bicarbazolyl-ene-alt-phenylenebis(cyanovinylene)[13] have been reportedvia the Knoevenagel reactions [14-16].

In addition to giving the polymers the properties described above, the nitrile groups provide the possibility of introducing tetrazole units, these groups are known by their basic and acidic character, as well as by their post-functionalization reaction.

Indeed, the cycloaddition reaction between nitriles and azides effectively leads to the corresponding 5-substituted 1*H*-tetrazoles, this reaction has been described as early as 1901 [17]. However, it was much less exploited than the azide-alkyne cycloaddition [18],including in the field of polymers [19].For example, post-polymerization azide-nitrile cycloaddition was used to prepare different molecular weight poly(5-vinyltetrazole) from polyacrylonitrile [20,21],polymer nanosieve membranes for CO_2-capture application [22] or membranes for ultrafiltration application [23].

In this context, in continuation of our previouswork on the preparation and studies on side chain isosorbide-containing poly(p-phenylenevinylene)s [24],herein,we describe the synthesis and physical properties of a new isosorbide-substituted cyano-paraphenylene vinylene polymer precursor (**CN-PPVIs**) as well as the corresponding isosorbide- and tetrazole-containing side chain polymer (**Tet-PPVIs**) efficiently obtained *via***Click chemistry** post-functionalization reaction between nitriles and sodium azide.

II. Experimental section

2.1 Reagents

All the reagents and solvents were used according to commercial availability (Acros organics France)**.**

2.2 Methods

spectroscopic techniques

NMR:proton and Carbon-13 Nuclear magnetic resonance (^{1}H NMR and ^{13}C NMR) wereobtained with a Bruker AV 300 spectrometer (Biospin, Strasbourg, France).

FTIR: Fourier transform infrared (FT-IR)spectra were recorded on a Perkin-Elmer BX FTIR (Perkin-Elmer, California, USA) system spectrometer by dispersing samples in KBr disks.

Ultraviolet-visible absorption:UV-vis absorption spectra were recorded on a Cary 300 spectrophotometer (Agilent, France).

PL: photoluminescence (PL) spectra were obtained on a Jobin-Yvon spectrometer HR460 (HORIB, Kyoto, Japan)coupled to a nitrogen-cooled Si charged-coupled device (CCD).

The PL quantum yield was determined in dilute chloroform solution using quinine sulphate (10^{-5} M solution of 0.5 H_2SO_4).

the PL quantum efficiency of the sample (Φ_s) was calculated using the following equation:

$$\Phi_s / \Phi_r = (A_r/A_s)\,(F_s/F_r)\,(n_s^2/n_r^2)$$

with A_r is the absorbance at the excitation wavelength ; F_r is the emission integration area for the reference ; A_s is the absorbance integral for the sample ; F_s is the emission integral for the sample; $n_s$are the refractive index of the polymer solution and n_r is the refractive index of quinine sulfate solution.

Chromatographic technique

SEC: Size exclusion chromatography (SEC)was performed on an Agilent Technologies 1200 HPLC (Agilent, France).

Thermal analysis

DSC: Differential Scanning Calorimetry (DSC) was performed on a Mettler Toledo DSC (Mettler Toledo, France) with a heating rate of 10 °C min^{-1}.

TGA: Thermogravimetric analysis (TGA) was carried out on TA Instruments Q50 (TA Instruments, USA) under nitrogen at a heating rate of 10 °C min^{-1}.

Electrochemical analysis

CV: Cyclic voltammetry (CV) was performed on a CHI 660B electrochemical station.

Measurements were performed at a scan rate of 50 mV s-1 with a three-electrode cell (Ag/AgCl as reference electrode, a platinum counter electrode and indium tin oxide (ITO/1cm^2) as working electrode) using a solution of tetrabutylammonium fluoroborate ((n-Bu)4NBF4) in 0. 1 M in acetonitrile as supporting electrolyte.

Fabrication and characterization of diodes

The single-layer device was developed as sandwich structures between an aluminium (Al) cathode and an indium tin oxide (ITO) anode - 100 nm thick, 20 Ω/square sheet resistance. The ITO substrate was supplied by Merck Display Technologies (MDT) and partially etched to avoid short circuits.

After the engraving process, the ITO substrate was successively pre-cleaned in acetone and isopropyl alcohol. The polymer solution (2.10^{-2} M in chloroform) was spin-coated at 2000 rpm for 1 min onto the ITO glass electrode to obtain a film thickness of about 60 nm, determined by an Alpha-Step IQ profilometer.

A thin layer of aluminium (150 nm, aluminium surface area approx. 10 mm^2) was deposited by thermal evaporation under a vacuum of 3.10-6 Torr at speeds of 1 nm/s. Electrical transport measurements were made using a Keithley 236 source unit and impedance spectroscopy measurements were recorded using an HP 4192 LF impedance analyser.

All electrical measurements were performed in the dark, at room temperature and atmosphere. The electrical results are reproducible after successive scans and for several months without special storage conditions.

2.3 Synthesis of intermediaries and Monomers

As can be seen in Scheme 1, compound **a** was synthesized from isosorbide in 5 steps, then monomer $\mathbf{M_1}$ was obtained by the reaction of compound **a**into three steps, in fact the detailed protocol for the synthesis of these two compounds is outlined in our previous work [25].

Synthesis of 1,4:3,6-dianhydro-2-O-hexyl-5-[3,6-cyanomethyl-4-methoxyphenyloxy]-5-deoxy-L-iditol ($\mathbf{M_2}$)
A solution of **a** (7.5 mmol) and potassium cyanide (30 mmol) in DMF (15 mL) was stirred at room temperature for 6 hours. The resulting mixture was then poured into distilled water; the precipitate was filtered, washed with water and dried under vacuum. The residue was purified by recrystallization from ethanol to give of $\mathbf{M_2}$ as a white powder (75%). M.p: 76°C;**^{1}H NMR** (300 MHz, $CDCl_3$, δ): 6.99 (s, 1H, Ar-**H**), 6.94 (s, 1H, Ar-**H**),4.8-4.79 (m, 1H, $\mathbf{H_5}$), 4.69 (m, 2H, $\mathbf{H_2}$, $\mathbf{H_3}$), 4.07-3.87(m, 8H, $\mathbf{H_1^a}$, $\mathbf{H_4}$, $\mathbf{H_6^{a,b}}$, C$\mathbf{H_2}$CN), 3.75-3.61 (m, 4H, H_1^b, OC$\mathbf{H_3}$), 3.55-3.49 (m, 2H, -OC$\mathbf{H_2}$), 1.61 (q, ^{3}J= 6.9 Hz, 2H, OC$\mathbf{H_2}$C$\mathbf{H_2}$)), 1.36-1.3 (m, 6H, **OC**H_2**C**H_2**(CH_2)$_3$)**, 0.89 (t, ^{3}J= 6.6 Hz , 3H , -C$\mathbf{H_3}$);
^{13}C NMR (75 MHz, $CDCl_3$, δ):150.94, 147.43, 119.73, 119.02, 116.95, 116.91, 113.77, 111.62, 85.50, 84.77, 82.85, 81.74, 71.95, 71.27, 69.49, 55.64, 31.10, 29.18, 25.22, 22.06, 18.29, 18.19, 13.50;**FTIR** (cm^{-1}): 3070 (w, aromatic C-H stretching),2250 (s, C-CN stretching), 1449 (s, C=C stretching), 822 (s, aromatic C-H out-of-plane bending).

2.4 Preparation of the isosorbide-based polymers type PPV

Synthesis of the cyano-Polymer: CN-PPVIs
The synthesis of polymer **CN-PPVIS** was accomplished using Knoevenagel condensation[26].To a solution of dialdehyde $\mathbf{M_1}$ (1.5 mmol) and $\mathbf{M_2}$ (1.5 mmol) in freshly prepared anhydrous THF (6.25 mL) and methanol (3 mL) under a nitrogen atmosphere was added dropwise 0.9 mL of a 1 M solution of $(Bu)_4NOH$ in methanol. The mixture was vigorously stirred and heated at reflux for 12 hours. The resulting mixture was then cooled to room temperature, poured into water, and extracted with chloroform. The organic phase was washed with water, partially concentrated and then precipitated into methanol to afford **CN-PPVIs** as a red powder (70%). **FTIR** (cm^{-1}): 3045 (w, aromatic and vinylic C-H stretching), 2928-2859 (w, aliphatic C-H stretching), 2209 (s, CN stretching), 1505 (m, C=C stretching), 1208 (s, C-O-C asymmetric stretching), 1095 (s, C-O-C symmetric stretching), 918 (m, *E*-HC=CH out-of-plane bending), 861 (w, *Z*-HC=CH out-of-plane bending), 783 (s, aromatic C-H out-of-plane bending); **^{1}H NMR** (300 MHz, $CDCl_3$, δ): 8.19-6.50 (m, aromatic and vinylic protons), 4.89-3.47 (m, $\mathbf{H_1}$, $\mathbf{H_2}$, $\mathbf{H_3}$, $\mathbf{H_4}$, $\mathbf{H_6}$, OC$\mathbf{H_2}$, OC$\mathbf{H_3}$), 1.55-0.87 (m, $OCH_2(CH_2)_4$), C$\mathbf{H_3}$);
Synthesis of the tetrazole based-Polymer: **Tet-PPVIs**
To a solution of **CN-PPVIs** (1 mmol)in DMF (5 ml) and NaN_3 (3 mmol) was added $ZnBr_2$ (3mmol), and the mixture was stirred at 150°C for 5 days. HCl (3 N, 30 mL) and ethyl acetate (100 mL) were added, and vigorous stirring was continued until no solid was present and the aqueous layer had a pH of 1. The organic layer was isolated and the aqueous layer extracted with 2 · 100 mL of ethyl acetate. The combined organic layers were concentrated, 200 mL of 0.25 N NaOH were added, and the mixture was stirred for 30 min, until the original precipitate was dissolved and a suspension of zinc hydroxide was formed. The suspension was filtered, and the solid washed with 20 mL of 1 N NaOH. To the filtrate was added 40 mL of 3 N HCl with vigorous stirring and extracted with ethyl acetate. The organic phase was washed with water, partially concentrated and then precipitated into methanol to afford **Tet-PPVIs** as a brown solid (50%). Elem. Anal. Calculated for $\mathbf{C_{44}H_{55}O_{10}N_5}$: N, 3.95%; Found: N, 3.86%; **FTIR** (cm^{-1}): 3400 (s, N-H stretching), 2200 (s, CN stretching), 1600 (s, N=N stretching); **^{1}H NMR** (300 MHz, $CDCl_3$, δ):8.00-6.50 (m, aromatic and vinylic protons), 4.90-3.20 (m, $\mathbf{H_1}$, $\mathbf{H_2}$, $\mathbf{H_3}$, $\mathbf{H_4}$, $\mathbf{H_6}$, OC$\mathbf{H_2}$, OC$\mathbf{H_3}$), 1.80-0.80 (m, $OCH_2(CH_2)_4$), C$\mathbf{H_3}$);

III. Results and discussion

3.1 Synthesis and characterization of the polymers

The strategy for the synthesis of polymers **CN-PPVIs** and **Tet-PPVIs** is described in Scheme 1.

Synthesis of monomers

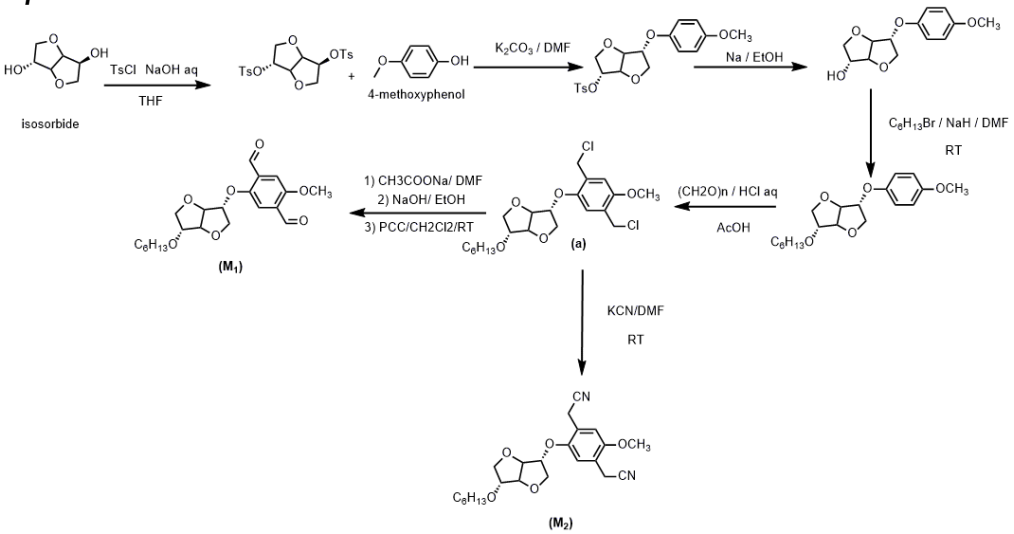

Synthesis of polymers

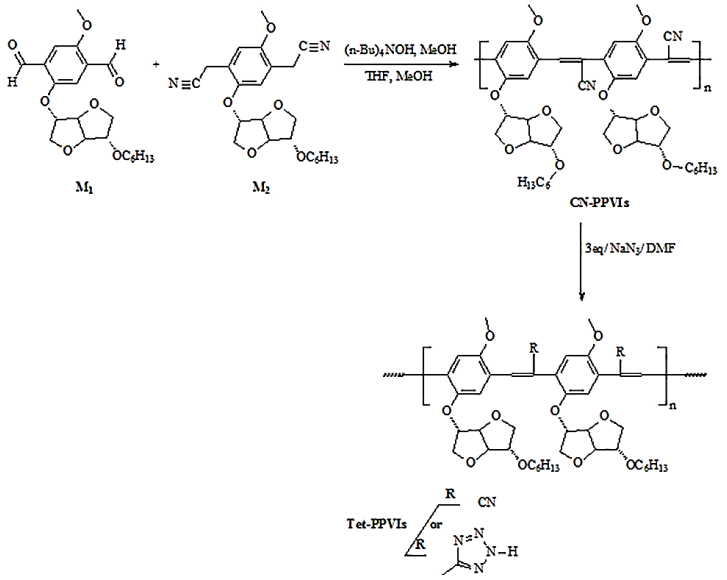

Scheme 1. Synthetic route to the polymers **CN-PPVIs** and **Tet-PPVIs**.

Herein, we took advantage of the isosorbide-based chloromethyl compound (**a**) that we described previously [24].

On the one hand, the monomer M_1 was obtained in two steps from intermediate **a**, on the other hand, monomer M_2 was obtained by a reaction of compound **a** with KCN in DMF at room temperature.[25]

These two functionalized monomers (M_1 and M_2) were then polymerized to afford CN-PPV derivative (**CN-PPVIs**)through a Knoevenagel condensation using tetra-*n*-butylammonium hydroxide as a base in a THF/MeOH mixture.

The tetrazole-modified PPV (**Tet-PPVIs**) was obtained by modification via Click chemistry reactionof **CN-PPVIs** as a precursor polymer.Indeed, this semi-conducting material was prepared by 1,3-dipolar cycloaddition between nitrile groups of **CN-PPVIs** and azide ions to incorporate tetrazole unitsin the macromolecular chain.

The two polymers are very soluble in common volatile solvents(Tetrahydrofuran, Chloroform, Methylene chloride) and show good film forming ability.

The polymer chemical structures were confirmed by NMR and FT-IR spectroscopic studies.

The ^{1}H NMR spectrum of polymer **CN-PPVIs** confirmed the presence of aromatic and vinylic protons, which gave signals between 8.20 and 6.50 ppm. The signals of OCH_2, OCH_3 groups and dianhydro protons appeared in the 4.90 and 3.20 ppm range, the aliphatic groups giving rise to a multiplet between 1.55 and 0.77 ppm. The absence of aldehyde protonwas also confirmed by the absence of signal to around 10 ppm.

The FT-IR spectrum of **CN-PPVIs** showed the presence of both *Z* (867 cm^{-1}) and *E* (969 cm^{-1}) vinylic configurations[27] as well as the cyano group that gave stretch absorption band at about 2200 cm^{-1}.

The ^{1}H NMR spectrum of polymer **Tet-PPVIs** was quite similar to that of **CN-PPVIs** but its FT-IR spectrum revealed an absorption band near 1600 cm^{-1} due to stretching vibration of the N=N and N–H groups, indicating that some of the nitrile groups were transformed into tetrazole groups. The CαN stretching vibration band at 2200 cm^{-1}always being present, which have demonstrated that the post-modification of **CN-PPVIs** was not quantitative.

Furthermore, the elemental analysis could also give an insight into the average molar ratio of the tetrazole formed in the **Tet-PPVI**, compared to the initial total of accessible nitrile groups in the polymeric **CN-PPVI**, was about 53%.

Finally, size-exclusion chromatography (SEC) analysis in THF allowed us to estimate the number-average molecular weights (Mn) in the range of 4500 and 4800 $g.mol^{-1}$ for **CN-PPVIs** and **Tet-PPVIs**, respectively and the dispersity (Đ) around 1.8.

The thermal behavior of the polymers was investigated by thermogravimetric analysis (TGA) and differential scanning calorimetry (DSC). The TGA thermograms, shown in Fig. 1, indicate a major degradation at 390°C for **CN-PPVIs** and 375°C for **Tet-PPVIs**, which suggest that tetrazole units are slightly less stable than nitrile groups. However, the DSC doesn't show any melting or other thermal manifestation,we could conclude that both polymers have an amorphous morphology in the solid state.

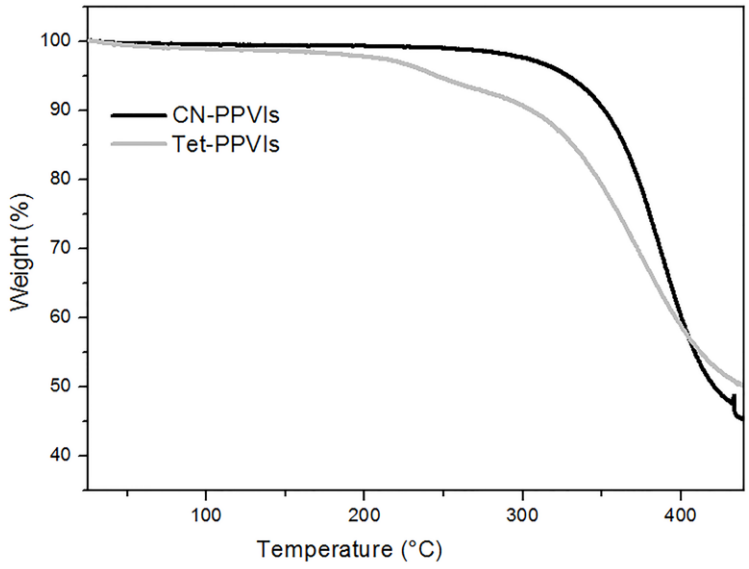

Fig. 1. TGA thermograms of polymers **CN-PPVIs** and **Tet-PPVIs**

3.2 Thin-film surface properties

The thin films were investigated by contact angle measurements, it is a convenient way to characterize the surface polarity, so it is an essential parameter for optimizing the polymer/metal interface in any potential electronic device application. More precisely, it has been demonstrated that increasing the polarity of the polymer active layer favors the interfacial adhesion with metal electrodes and prevents its crystallization, thus improving the charge carrier injection efficiency [28].

Moreover, it has been evidenced that the ground state dipole moment of the π-conjugated system shows an essential role in the carrier transport and the electroluminescent properties in OLEDs [29].Thus, the Van Oss-Chaudhury-Good model was exploited; using three test liquids (water, diiodomethane and formamide) [30],the obtained results are reported in Table 1.

In comparison with **CN-PPVIs**, the polymer containing tetrazole (**Tet-PPVIs**) showed considerably higher acid components. This behavior can be attributed to the presence of tetrazole groups in the macromolecular chain which have an acidic character.

Indeed, a higher polarity of the surface was obtained for **Tet-PPVIs** (Table 1). Moreover, **Tet-PPVIs** exhibit a more polar surface than the poly[2-methoxy-5-(2'-ethylhexyloxy)-1,4-phenylenevinylene](MEH-PPV), which presents a *P* value of 0.03 [31].

Table. 1 Surface characteristics of **CN-PPVIs** and **Tet-PPVIs**.

	γ^+	γ^-	γ^{AB}	γ^{LW}	γ^s	*P*
Glass surface	2.0	47.8	19.5	36.7	56.1	
CN-PPVIs	0.4	17.6	5.3	39.6	44.9	0.11
Tet-PPVIs	1.2	11.2	7.3	35.5	42.8	0.17

γ^+: acid energy component; γ^-: basic energy component ; $\gamma^{AB} = 2(\gamma^+\gamma^-)^{1/2}$:polar energy; γ^{LW}: apolar energy ; $\gamma^S = \gamma^{AB} + \gamma^{LW}$: surface energy; $P = \gamma^{AB}/\gamma^s$: polarity.

3.3 UV-vis absorption

The UV-Vis absorption properties of these new PPV derivatives were investigated at room temperature, in chloroform dilute solutions (5.10^{-5}M) and in thin solid films(2.10^{-2}M).

The obtained solution and filmabsorption spectra of the polymers are reported respectively in Fig.2 andFig. 3; their optical data are summarized in Table 2.

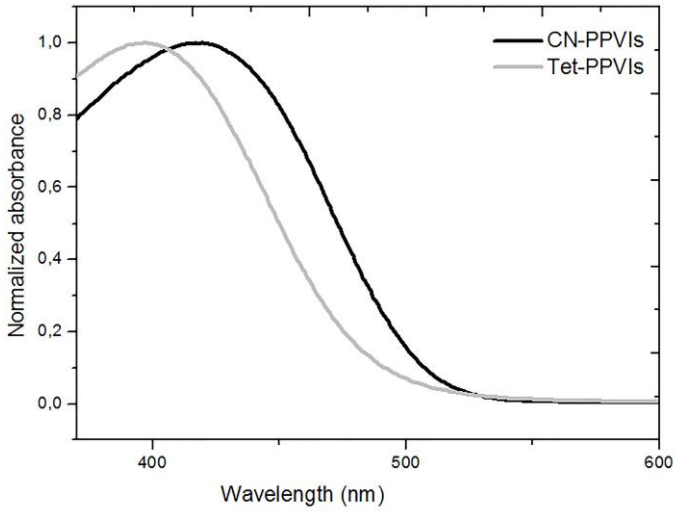

Fig. 2. UV-vis absorption spectra of polymers in chloroform solutions ($5{\cdot}10^{-5}$mol. L^{-1})

In dilute solution, the polymers absorption spectra show similar shapes but they present one maximum at 460 nm for **CN-PPVIs**(2.69 eV) and 395 nm (3.14 eV) for **TET-PPVIs,** respectively.

Furthermore, the onset of absorption in dilute solution of **Tet-PPVIs** was significantly blue-shifted (25 nm), indicating a lower efficiency of its conjugation length compared to **CN-PPVIs**.

This behavior may be due to the steric hindrance, created by the tetrazole groups, which affects the conformation of the conjugate system, reducing its flatness.

Note as well as thatin thin solid film, the **CN-PPVIs** spectrum was broader, and the absorption onset was significantly red-shifted (20 nm) in comparison with the dilute solution state.

In fact, similar behavior is generally observed in semi-conducting polymers and it was attributed to the π-π interaction of the conjugated segments and the formation of aggregates in the thin film [29].

However, going from dilute solution to thin film in the case of the Tetrazole-based polymer (**Tet-PPVIs**), we obtained nearly the same spectra, which indicated a very limited π-π interaction between the conjugated systems in the case of **Tet-PPVIs**, this is probably due to the volume occupied by the tetrazole units which could limit the macromolecular chainstacking in solid state.

The optical band gaps (Eg-op) were estimated from the absorption onsets of the polymer thin films. They are of 2.35 and 2.53 eV for **CN-PPVIs** and **Tet-PPVIs**, respectively. The resulting gap energies classified these synthesized polymers as organic semiconductors.

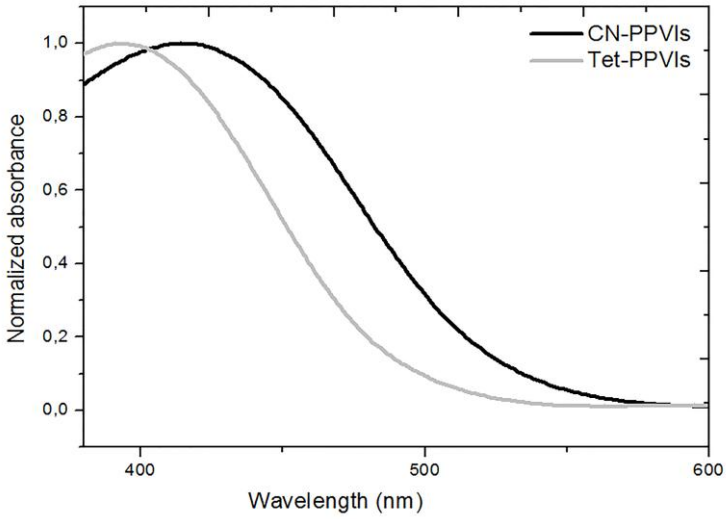

Fig. 3. UV-vis absorption spectra of polymer thin solid films (80 nm)

Table 2 UV-visible absorption data of **CN-PPVIs** and **Tet-PPVIs**.

	Dilute solution in chloroform				***Thin film***			
	λ_{max} (nm)	ε_{max} (10^4. $M^{-1}.cm^{-1}$)	FWHM[(a)] (nm)	λ_{onset} (nm)	λ_{max} (nm)	λ_{onset} (nm)	FWHM[(a)] (nm)	Eg_{-op} (eV)
CN-PPVIs	415	2.04	148	507	415	527	169	2.35
Tet-PPVIs	395	1.55	143	483	395	490	146	2.53

(a) Spectrum full width at half maximum

3.4 Photoluminescence properties

The photoluminescence properties of both polymersin dilute solution and in thin film were investigated at room temperature; the obtained spectra are presented in Fig. 4 andFig. 5. The photoluminescence data are summarized in Table 3.

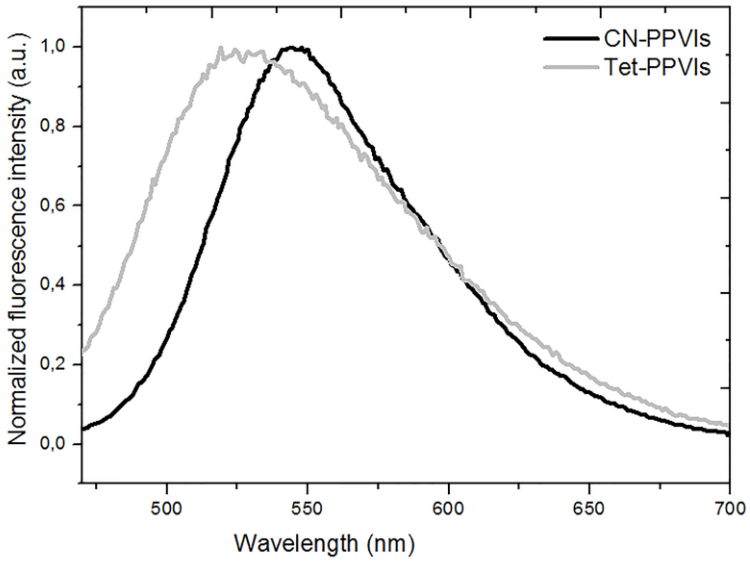

Fig. 4. Fluorescence spectra of polymer solutions (in chloroform, 2.10^{-7}mol. L^1)

Indeed, both polymers exhibit a green emission in dilute solution with one maximum, at 545 nm for **CN-PPVIs** and 525 nmfor **Tet-PPVIs**.

The fluorescence quantum efficiencies of thetwo polymers were determined in dilute chloroform by a relative method using quinine sulfate as a standard [32],leading to values of 60 % for **CN-PPVIs** and 45 % for **Tet-PPVIs**.

Table 3 Photoluminescence dataof **CN-PPVIs** and **Tet-PPVIs**.

	Dilute solution in chloroform			*Thin film*	
	λ_{max}(nm)	FWHM[(b)] (nm)	Φ_{fl}[(c)]	λ_{max}(nm)	FWHM[(b)] (nm)
CN-PPVIs	545	84	0.60	603	84
Tet-PPVIs	525	109	0.45	561	146

(a) Shoulder. (b) Spectrum full width at half maximum. (c) PL quantum yields

The lower quantum yield observed for **Tet-PPVIs** could be explained by the presence of tetrazole groups.
In fact, the available vibrational and rotational degrees of freedom are increased with the incorporation of these units and therefore the loss of PL through these processes is increased [33].
In solid-state, we observed that the fluorescence spectra of **CN-PPVIs** and **Tet-PPVIs** were significantly red shifted and broader, in comparison with its analogue in dilute solution (Fig. 5(a)).
As mentioned in thin film absorption studies, this behavior is ascribed to the π-π interaction of the excited conjugated systems and excimer formation in the solid state [34].
The chromaticity coordinates of the emitted fluorescence were illustrated on the 1931 CIE diagram in Fig. 5, which show a yellow-orange emission for **CN-PPVIs,** and an orange emission for **Tet-PPVIs**.

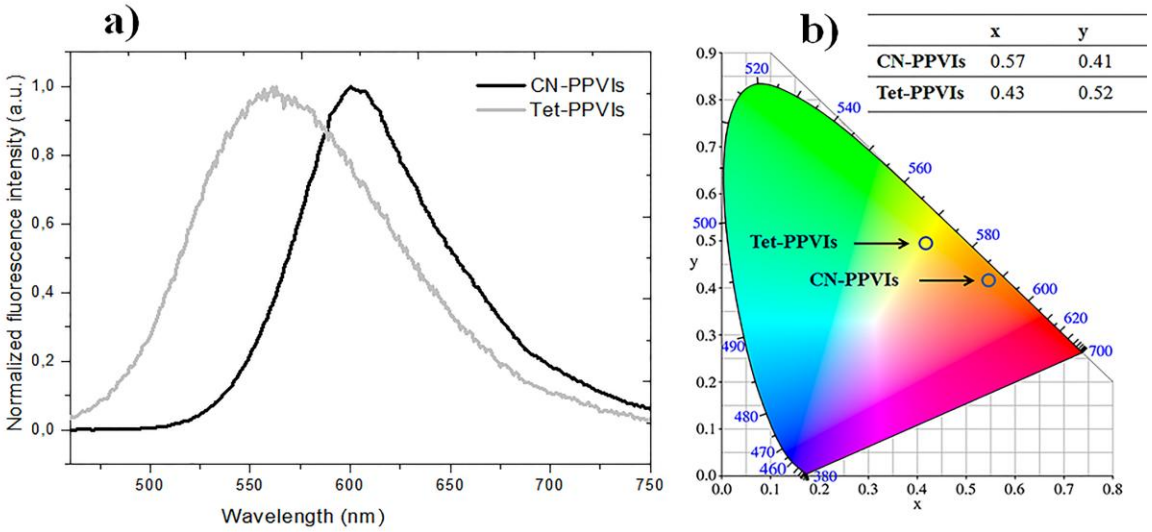

Fig. 5. (a) Fluorescence spectra of polymer thin films(80 nm);
(b) the CIE chromaticity diagram

3.5 Electrochemical characterization

The knowledge of the HOMO (highest occupied molecular orbital) and LUMO (lowest unoccupied molecular orbital) frontier energy levels is of crucial importance to determine energy barriers and select cathode and anode materials in order of making PLEDs [35].Similarly, these parameters are also of essential importance in optimizing the efficiency of charge-carrier photogeneration in polymeric solar cells, and charge injection in polymeric thin-film transistors [36].This is the reason why cyclic voltammetry (CV) analysis is reliable, as the electrochemical processes are similar to those involved in charge injection and transport processes in such electronic devices [37].

Thus, the HOMO and LUMO energy levels of our polymers were evaluated with this technique. The polymer films were drop-coated onto ITO glass substrates and studied by applying either positive or negative potentials in a 0.1 M $(n\text{-}Bu)_4NBF_4$/acetonitrilesolution at a scan rate of 50 mV s^{-1}.
According to a previously reported empirical method, and by assuming that the energy level of the ferrocene/ferrocenium is of 4.8 eV below the vacuum level, the frontier energy levels and the electrochemical gap ($E_{g\text{-}el}$) of the polymercould be calculated as follows [38]:

$$E_{HOMO} = -(V_{onset\text{-}ox} - V_{FOC} + 4.8)\ eV$$
$$E_{LUMO} = -(V_{onset\text{-}red} - V_{FOC} + 4.8)\ eV$$
$$E_{g\text{-}el} = (E_{LUMO} - E_{HOMO})\ eV$$

Where, V_{FOC} is the ferrocene half-wave potential (0.8 V), $V_{onset\text{-}ox}$ is the polymer oxidation onset and $V_{onset\text{-}red}$is its reduction onset, all measured being expressed versus Ag/AgCl (the reference electrode used in this work).
In comparison with polymer containing a CN group (CN-PPVIs), tetrazole-modified **Tet-PPVIs** displayed a lower ionization potential (*IP*)and a higher electron affinity(*EA*), as shown in Fig. 6,

This observation indicates that the electron injection ability has been enhanced by the introduction of the tetrazole moieties in the polymer backbone.

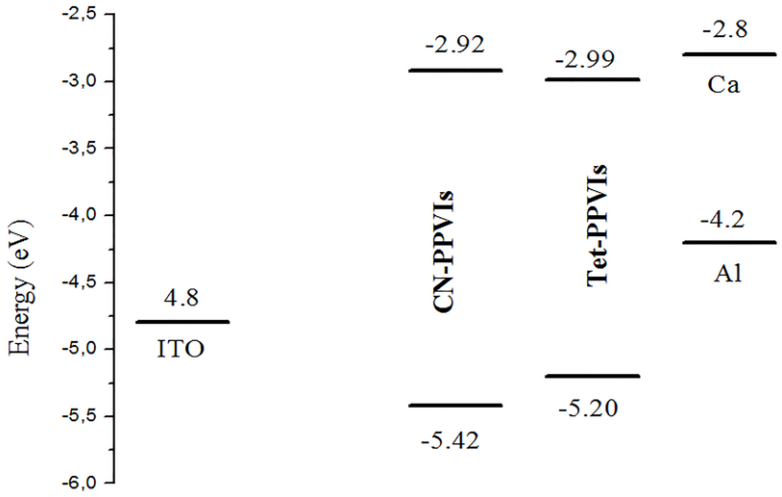

Fig. 6. Energy diagram of ITO, **CN-PPVIs**, **Tet-PPVIs** and Al.

3.6 Theoretical investigations

Geometry optimization and electronic properties of the investigated chemical structure

Quantum chemical computations were performed using density functional theory (DFT) implemented in the Gaussian 09 program [39]. Molecular geometries of the synthesized polymers were optimized in the ground state with PBE0 and B3LYP functional, combined with the 6-31G (d, P) basis set[40]. The optimization is done in gas phases. Electronic parameters such as E_{HOMO}, E_{LUMO} and energy gap $E_{H\text{-}L}$ of the optimized chemical structure are summarized in table 1, with the experimental energy gap for comparison.

From table 1, it is clearly seen that the DFT/PBE0/6-31G(d,p) level of theory reproduces the experimental energy gap. The optimized chemical structures of the synthesized molecules calculated with DFT/PB0/6-31G(d,p) are represented in Fig7.

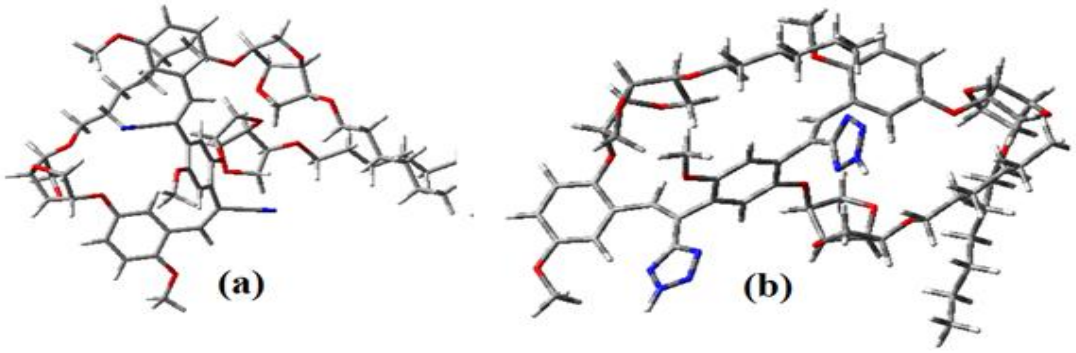

Fig.7. DFT/PBE0/6-31G(d,p) optimized chemical structure of **CN-PPVIs** and **Tet-PPVIs**.

Table 4. Calculated electronic parameters of the **CN-PPVIs** and **Tet-PPVIs**.

		DFT/B3LYP/6-31G(d,p)	DFT/PBE0/6-31G(d,p)	Dipole moment μ(D)*	Experimantal E_{H-L} (eV)
CN-PPVIs	**HOMO**	-5.4	-4.56	**4**	**2.53**
	LUMO	-1.83	-2.53		
	E_{H-L}	**3.56**	**2.02**		
Tet-PPVIs	**HOMO**	-5.09	-4.26	**2**	**2.21**
	LUMO	-1.165	-2.11		
	E_{H-L}	**3.9**	**2.15**		

*** calculated μ(D) at the ground state by DFT/PBE0/6-31G(d,p)**

Based on the DFT/PBE0/6-31G(d,p) optimized chemical structure, the contour plots of the frontier orbitals HOMO and LUMO obtained with the isovalue of 0.02 are visualized using gaussview software [41]. Furthermore, the electronic structures of the investigated molecules are deduced using GAUSSSUM software[42] and the DOS of the investigated molecules are presented in Fig. 8.

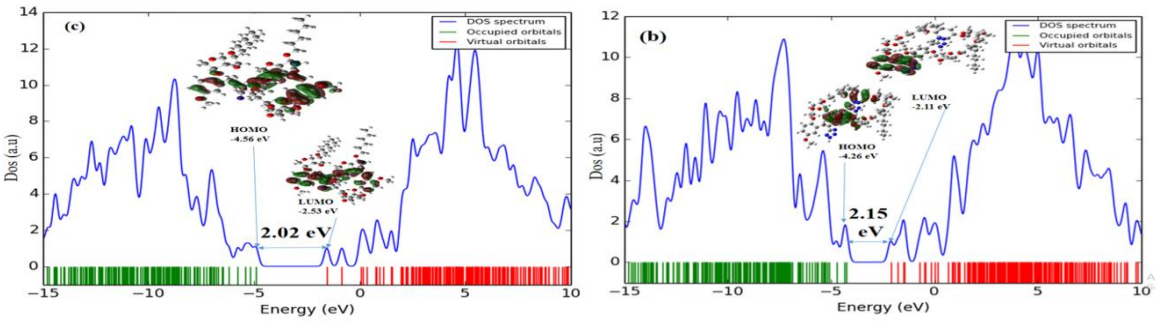

Fig. 8. Dos analysis of the chemical structure of **CN-PPVIs** and **Tet-PPVIs**.

The change of the insert chemical groups induces a change in their geometric properties, as well as electronic structure is greatly modified. Else, the contour plot HOMO and LUMO distribution change. In fact, the presence of cyano groups in the case of **CN-PPVIs** induces orbital distribution on the backbone of the polymer. Else, the insertion of tetrazole groups induces a local localization of HOMO and LUMO orbitals. Furthermore, the partial modification of cyano groups by Tetrazole ones exhibits a modification on the electronic parameters (see Table 1), and the calculated dipole moment decreases from 2 D to 4 D as a result of the geometric and electronic change.

Theoretical study of the non-covalent induced intramolecular interaction (RDG investigations).

In order to evaluate the type of the possible intramolecular interaction on the synthesized polymers Reduced Density Gradient (RDG) analysis was employed using VMD software and presented in Fig.9.

The color-coded map of RDG indicates high repulsion interaction due to steric effect (red colors), stronger interaction due to Hydrogen bonding (blue color), and intermediate interaction type Van der Waals (the green color).

From Fig. 9, we can deduce the absence of strong interaction or high hydrogen bonding on the two chemical structures. Meanwhile, the presence of oxygen atoms induces the formation of partial green to red halfelliptical slabs between aromatic rings shown in the iso-surface density maps. The formed slabs are more important in the structure containing tetrazole groups than containing cyano groups revealing that tetrazole sequence induces more medium Vander walls interaction and more strong repulsion on the chemical structure. Indeed, this behavior can confirm the experimental results in absorption. The presence of the greater repulsions in the case of **Tet-PPVIs** induces a torsion at the level of the conjugate system and decreases the effective length of the conjugation. It can therefore be concluded that the steric effect outweighs the attracting effect of the tetrazolegroup in this type of organic material.

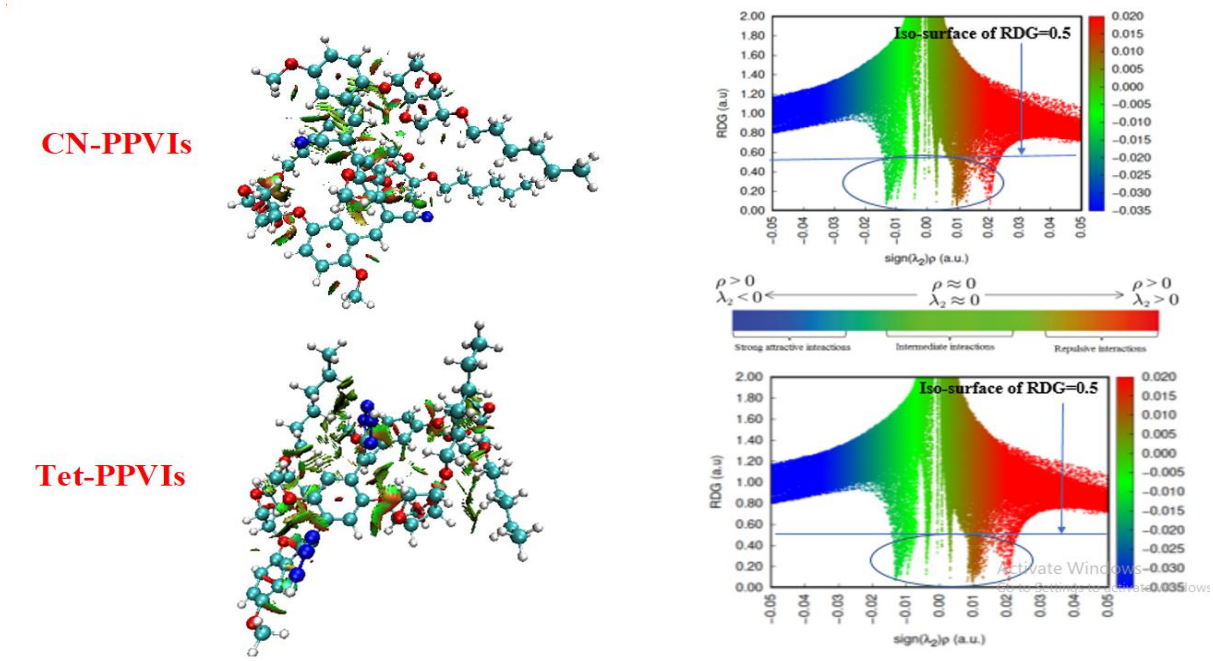

Fig. 9. (Right) Non-Covalent Interaction (NCI) scatter diagram and (Left) Reduced Density Gradient (RDG) analysis of **CN-PPVIs** and **Tet-PPVIs**. investigated structure.

3.7 Electrical characterization

The charge transports in the twopolymers have been investigated by current-voltage measurements, at room temperature as shown in Fig. 10(a).

The [ITO/ **polymer**/Al] devices were operating in both forward and reverse bias modes and showed typical diode behavior with a threshold bias of 2.55 V for **CN-PPVIs** and 4.01 for **Tet-PPVIs**.

Thus, the dynamic resistances (R_d), turn-on voltages (V_{seuil}) and rectifying ratios (R_r) could be extracted from the J-V characteristics and are presented in Table 5.

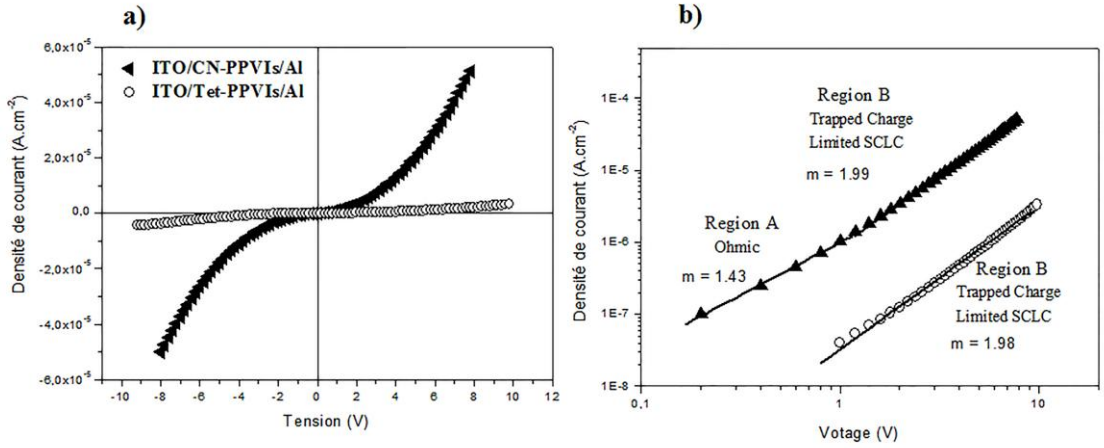

Fig. 10. The J-V characteristics for the [ITO/**Polymer**/Al] diodes: (a) in linear representation; (b) in log-log representation.

Table 4. Electrical parameters for the [ITO/Polymer/Al] devices, derived from *J-V*characteristics

	CN-PPVIs	**Tet-PPVIs**
Turn-on voltage, V_{seuil}(V)	2.55	4.01
Rectification ratio, R_r	1.27	0.45
Dynamic resistance, R_d(kΩ)	458	4761
Mobility, μ_{eff} ($cm^2.V^{-1}.s^{-1}$)	3.77 10^{-8}	1.44 10^{-9}

The current dependence of applied voltage appears to follow the power law $J \alpha V^m$, as revealed by the log-log presentation of the *J-V* characteristic in Fig. 10(b).
Moreover, three regimes were observed and can be described as follows:
(A) An ohmic regime at low voltages, where the current depends linearly on the bias voltage (m = 1). In this case, the current density is given by [43]:

$$J_{\Omega} = q.p_0.\mu.\frac{V}{d} \qquad (1)$$

Where, q is the electronic charge, μ is the charge carrier mobility, p_0 is the free carrier density and d is the film thickness.
(B) At medium voltage, the current density depends quadratically on the voltage ($m = 2$). This region can be well explained using the space-charge limited current (SCLC) theory for trap-containing organic materials. The SCLC is limited by charge trapping and the current density is expressed by the relation [44]:

$$J_{SCLC} = \frac{9}{8}.\varepsilon.\mu_{eff}.\frac{V^2}{d^3} \quad (2)$$

Where, ε is the permittivity of the organic material (assumed to be $4\varepsilon_0$; ε_0 is the permittivity of vacuum). The μ_{eff} is the effective carrier mobility which is equal to $\theta\mu$, where θ is the fraction of free charge ($\theta = p/(p + p_t)$; p and p_t are the densities of free and trapped charges, respectively).
(C) At higher voltages, a trap filled SCLC with $J \alpha V^7$ was measured.
Indeed, a further increase in voltage will result in the introduction of free carriers that cannot be trapped again and consequently the current will intensify rapidly. The hole effective mobility (μ_{eff}) in the polymer films were estimated by fitting the *J-V* characteristic to the SCLC model and were of 3.77 10^{-8} $cm^2.V^{-1}.s^{-1}$ for **CN-PPVIs** and 1.44 10^{-9} $cm^2.V^{-1}.s^{-1}$ for **Tet-PPVIs**.

IV.Conclusion

A novel polymer containing isosorbide-type polar side chain and including about 50% of tetrazole-units (**Tet-PPVIs**) was efficiently synthesized by click chemistry (cyano-tetrazole conversion) of a corresponding cyano-PPV type polymer (**CN-PPVIs**). The tetrazole-containing polymer (**Tet-PPVIs**) had a better solubility in polar solvents in respect to **CN-PPVIs** and exhibited good film-forming abilities, even if both these semi-conducting materials were amorphous and presented a good thermal stability. The optical properties of **CN-PPVIs** and **Tet-PPVIs** were investigated by UV-vis absorption and photoluminescence spectroscopies. Indeed, both polymers exhibited a green fluorescence in dilute solution with fluorescence quantum yield of 60 % for **CN-PPVIs** and 45 % for **Tet-PPVIs**. However, a blue-shift for absorption and fluorescence spectra was observed following the incorporation of the tetrazole units, indicating a lower effective conjugation length in the case of **Tet-PPVIs** in comparison with CN-polymer (**CN-PPVIs**). This result was confirmed theorical study. Moreover, the presence of tetrazole units in the macromolecular structure of **Tet-PPVIs** seems to limit the π-π interaction between the conjugated sequences and the aggregate formation in thin solid film. Finally, the HOMO/LUMO energy levels were evaluated by cyclic voltammetry measurements and indicated as expected a *p*-type semi-conducting behavior. In addition, the incorporation of tetrazole units in **Tet-PPVIs** lowered the ionization potential and increased its electronic affinity, allowing us to give preliminary results with ITO/polymer/Al configuration devices which show typical diode behavior with relatively low turn-on voltages. The study of the ITO/polymer thin film/Al devices showed a space-charge limited current transport mechanism with charge carrier mobility in order of 10^{-8} $cm^2.V^{-1}.s^{-1}$. The results obtained from the investigation of tetrazole-containing isosorbide-based polymers confirm that the incorporation of tetrazole moieties in PPV-conjugated system is a promising strategy to control the solubility, polarity, π-π interaction in thin film, HOMO-LUMO energy levels of conjugated polymers without reducing their photo-physical performance.

Acknowledgements

This study was funded by the Ministry of Higher Education and Scientific Research-Tunisia:
Laboratory of Advanced Materials and Interfaces (LR-11-ES-55).

References

[1]. T. ChatterjeeandK.-T.Wong,*Adv. Opt. Mater*.**2019**, *1*, 1800565.
[2]. S. Ashok Kumar, J.S. Shankar,B.K.Periyasamy, S.K. Nayak, *Polym.-Plast. Technol. Mater*.**2019**, *58*, 1–28.
[3]. B. Van der Zee, Y. Li, G.-J. A. H. Wetzelaer, and P. W. M. Blom, *Adv.Mater*.**2022**,*34*,2108887.
[4]. J. Cornil, D. Beljonne, D.A. Dos Santos and J.L. Bredas, *Synth. Met*.**1996**, *76*, 101-104.
[5]. J.Banerjee, K. Dutta, *Chem. Pap*.**2021**, *75*, 5139-5151.
[6]. C. A. Young, A. Hammack, H. J. Lee, H. J, T. Yu, M. D. Marquez, A. C. Jamison, B. E. Gnade, and T. R. Lee, *ACS Omega*. **2019**, *4*, 22332–22344.

[7]. S. P.O. Danielsen, C. R. Bridges, R. A. Segalman, *Macromolecules*.**2022**, *55*, 437-449.
[8]. G. Ahumada, and M. Borkowska,*Polymers*.**2022**, *14*,1118.
[9]. Y.Lin, J.Wang, Z.-G. Zhang, H.Bai, Y.Li, D. Zhu, X. Zhan,*Adv. Mater.***2015**, *27*, 1170–1174.
[10]. F. Wang, Y. Liu, X. Wan, J. Zhou, G. Long and Y. Chen, *Macromol. Chem. Phys.***2010**, *211*, 2503-2509.
[11]. M.R. Pinto, B. Hu, F.E. Karasz and L. Akcelrud, *Polymer*.**2000**, *41*, 2603-2611.
[12]. K. H. Au-Yeung, T. Kühne, D. Becker, M. Richter, D. A. Ryndyk, G. Cuniberti, T. Heine, X. Feng, F. Moresco, *Chem. Eur. J*.**2021**, *27*, 1-5.
[13]. J. Roncalli, *Chem. Rev*.**1997**, *97*, 173-206.
[14]. S. Xu, Y. Li, B. P. Biswal, M. A. Addicoat, S. Paasch, P. Imbrasas, S. Park, H. Shi, E. Brunner, M. Richter, S. Lenk, S. Reineke, X. Feng, *Chem. Mater*.**2020**, *32*, 7985-7991.
[15]. D. Becker, B. P. Biswal, P. Kaleńczuk, N. Chandrasekhar, L. Giebeler, M. Addicoat, S. Paasch, E. Brunner, K. Leo, A. Dianat, G. Cuniberti, R. Berger, X. Feng, *Chem. Eur. J*. **2019**, *25*, 6562-6568.
[16]. M. Di Giovannantonio, G. Contini, *J. Phys. Condens. Matter.***2018**, *30*, 093001.
[17]. A. Hantzsch and A. Vagt, *Liebigs Ann.***1901**, *314*, 339-369.
[18]. Z.Geng, J. J. Shin, Y. Xi, C. J. Hawker,*J.Polym. Sci.* **2021**, *59*, 963–1042.
[19]. K. Cho, H-S. Yang, I-H. Lee, S. M. Lee, H. J. Kim, and S. U. Son, *J. Am. Chem. Soc.***2021**,*143*, 4100−4105.
[20]. M.R. Huang, X.G. Li, S.X. Li and W. Zhang, *React. Funct. Polym.***2004**, *59*, 53-61.
[21]. N.V. Tsarevsky, K.V. Bernaerts, B. Dufour, F.E. Du Prez and K. Matyjaszewski, *Macromolecules*.**2004**, *37*, 9308-9313.
[22]. N. Du, H.B. Park, G.P. Robertson, M.M. Dal-Cin, T. Visser, L. Scoles and M.D. Guiver, *Nat. Rev*.**2011**,*10*, 372-375.
[23]. W. Zhao, L. Liu, L. Wang and N. Li, *RSC Ad.* **2016**, *6*, 72133-72140.
[24]. H. Zrida, K. Hriz, N. Jaballah, N. Sakly, D. Kreher and M. Majdoub, Express Polym Lett.**2014**,*8*, 709-722.
[25]. H. Zrida , K. Hriz, N. Jaballah, H. Hrichi, D. Kreher and M. Majdoub, *J. Mater. Sci*.**2016**, *51*, 680-693.
[26]. B. Ben Salem, K. Hriz, N. Jaballah, D. Kreher and M. Majdoub, *Opt. Mater.* **2015**, *50*, 114-122.
[27]. P.F.Van Hutten, V.V. Krasnikov, H.J. Brouwer and G. Hadziioannou, *J. Chem. Phys.* **1999**, *24*,139-154.
[28]. M. Petrosino, A. Rubino, *Synth. Met.***2012**, *161*, 2714-2717.
[29]. E. Gondek, J. Niziol, A. Danel, P. Szlachcic, K. Plucinski, J. Sanetra and I.V. Kityk, *Spectroc. Acta A.***2010**, *75*, 1501-1505.
[30]. C.J. Van Oss, M.K. Chaudhury and R.J. Good, *J Colloid Interface Sci*.**1987**, *28*, 35-64.
[31]. L. Feng and Z. Chen, *Polymer*.**2005**, *46*, 3952-3956.
[32]. W. H. Melhuish, *J. Phys. Chem. A.*, **1961**, *65*, 229-235.
[33]. N. Jaballah, M. Chemli, K. Hriz, J. L. Fave, M. Jouini and M. Majdoub, *Eur. Polym. J*.**2011**, *47*, 78-87.
[34]. K.Y. Peng, S.A**1983**. Chen, W.S. Fann, S.H. Chen and A.C. Su, *J. Phys. Chem. B.*, **2005**, *109*, 9368-9373.
[35]. B. Fan, Q. Sun, N. Song, H. Wang, H. Fan and Y. Li, *Polymer. Adv. Tech.***2006**, *17*, 145-149.
[36]. Y. Shirota and H. Kageyama, *Chem Rev*.**2007**, *107*, 953-1010.
[37]. M. Cheng, Y. Xiao, W.L. Yu, Z.K. Chen, Y.H. Lai and W. Huang, *Thin Solid Films*, **2000**, *363*, 110-113.
[38]. J.L. Bredas, R. Silbey, D.S. Bordeaux and R.R. Chance, *J. Am. Chem. Soc.**1983,105*, 6555-6559.
[39]. Y. Zhao, D.G. Truhlar, *Chem. Acc*.**2008**, *120*, 215–241.
[40]. S. Pesant, P. Boulanger, M. Côté, M. Ernzerhof, *Chem. Phys. Lett*. **2008**, *450*, 329–334.
[41]. R. Dennington TK, J. Millam,.GaussView, Version 5, Semichem Inc, Shawnee Mission KS 2009.
[42]. M. O'Boyle, A.L. Tenderholt, K.M. Langner, cclib: a library for package-independent computational chemistry algorithms, *J.Comput. Chem.***2008**, *29*, 839-845.
[43]. M.A. Lampert and P. Mark, Academic Press, New York, 1970.
[44]. K.C. Kao and W. Hwang, Pergamon Press, Oxford, 1981.

Habiba Zrida, et. al. "Isosorbide based-PPV derivatives containing electron-rich group for optoelectronic applications." *IOSR Journal of Applied Chemistry (IOSR-JAC),* 15(07), (2022): pp 23-35.